

Effects of Design Parameters on the Tip Steering Capabilities of Fabric Pneumatic Artificial Muscle-actuated Soft Growing Robots

Mario Selvaggio¹, Stanislao Grazioso², Salvatore Fusco², Roberto Sabella², Giuseppe Andrea Fontanelli³, Giuseppe Di Gironimo², Bruno Siciliano¹, and Antonio Lanzotti²

¹ Department of Electrical Engineering and Information Technology
Università degli Studi di Napoli Federico II
Via Claudio 21, 80125, Napoli, Italy

Corresponding author e-mail: mario.selvaggio@unina.it

² Dipartimento di Ingegneria Industriale
Università degli Studi di Napoli Federico II
P.le Tecchio 80, 80125, Napoli, Italy

³ Herobots S.R.L.
Traversa Vecchie Fontanelle 6, 80053
Castellammare di Stabia, Napoli, Italy

Abstract. Tip steering by induced deformation constitutes one of the most prominent feature to effectively navigate constrained environments with soft growing robots. In this work, we analyze the effects of design parameters on the tip steering capabilities of pneumatically-actuated soft growing robots built from fabric. More specifically, we consider the variability of material, fabric Pneumatic Artificial Muscles (fPAM) diameter, and backbone internal pressure and statistically quantify the effect on the maximum curvature achieved by the robot when a constant fPAM input pressure is applied. In our considered settings, we found a statistically significant main effect ($p < 0.05$) of the fPAM diameter and a relevant interaction effect between this and the material factor. These findings provide useful guidelines for the design of fabric-based PAM-actuated soft growing robots with enhanced tip steering capabilities.

Keywords: Soft Robotics; Soft Actuators; Design of Bioinspired Soft Robots

1 Introduction

In the recent years, the research and development of soft robotics solutions has undergone a tremendous growth [24, 8]. Due to their inherent compliance, soft robots are able to squeeze and safely absorb impacts that would crash their rigid-body counterpart. These capabilities constitute essential requirements in unstructured, uncertain and constrained environments where the interaction with the (most of the times unknown) surrounding is unavoidable.

Soft growing or *vine-inspired* robots imitate plant-like growth to change their body length and navigate through confined spaces [18]. Besides being inherently soft, they can navigate without sliding through constrained environments [14], possibly creating structures with their body [7]. Soft growing robots utilize the eversion of a thin-walled tubular structure to grow their body by continuously supplying material to their tip. To date, vine robots have been utilized to design proof-of-concept soft catheters for low-force interactions in constrained surgery [26], millimetre-scale medical devices to detect invasive breast cancers [3] or for endovascular surgery [20], re-configurable and deployable antennas [4], root-like burrowing robots [23], and inspection devices deployed in archaeological sites in South America [9].

Soft growing robots can steer themselves to effectively navigate cluttered and constrained environments by safely exploiting interactions with obstacles [15] or soft actuators embedded along the main robot body (hereafter denoted to as backbone). Several actuation mechanisms have been proposed so far: series pouch motors [16, 13], integrated pouches [1], inextensible elements attached to the main robot body [6], pre-formed tubes [26], and tendons [27], which are sometimes utilized in combination with stiffening [11] and shape-locking mechanisms [28]. Among these, fabric Pneumatic Artificial Muscles (fPAM) have been shown to be one of the most promising solution [22]. They are usually made of a thin, thus foldable and highly conformable, silicone coated ripstop nylon fabric and behave like a McKibben muscle when pressurized, but have no sheath friction. They have been shown capable of repeatable, near-linear force-contraction relationship, and exhibit fast dynamic response and high fatigue life [22]. Thus, they have been used to effectively steer a soft growing robot through an environment cluttered with obstacles by contracting the sides of the robot's backbone [25].

The development of model-based control techniques for navigation by growing and steering of vine robots is challenged by the complex behavior they exhibit. Accurate models require a characterization of the soft growing robot to establish the relation between the control inputs and the resulting system dynamic evolution and final configuration [2]. For example, establishing the relation between the fluid input pressure and the eversion rate of the backbone can be useful to avoid overshoot in a lengthening regulation problem. This represents a key issue since retraction is still difficult to be carried out due to complicated effects, such as buckling [21]. Solutions to this problem are currently under development [10][19]. To tackle the control problem, most of the prior works rely on simplified kinematic or dynamic models which are usually identified on purpose [5, 17]. Moreover, external loads such as gravity or (typically unknown) obstacle interactions modify these relationships further complicating the matter [29].

However, the effects of the (usually imperfect) design and fabrication parameters on the robot performance have never been quantitatively established and are only limitedly known to experienced manufacturers. None of the above works have, indeed, experimentally identified and analyzed the combined effect

of both *design* and external *actuation* parameters on soft growing robots’ motion capabilities, in particular those related to their tip steering.

This work carries out the characterization of fPAM-actuated soft growing robots, in terms of finding out the relationships among their design parameters, actuation inputs and the resulting tip steering capabilities of the robot. These are quantified by the maximum deformation the robot is capable to exhibit when actuated, and constitutes the second most the prominent feature to effectively navigate constrained environments, besides growing. More in details, we establish the relation between fPAM input pressure and the resulting constant curvature steering deformation of the whole robotic structure and analyzed which are the effects of fPAMs diameter, backbone and fPAM material, and backbone stiffness on this metric. Differently to what stated in [22], we found that the fPAM relationship between the input pressure and the muscle contraction is similar to what can be observed in McKibben muscles [12] but it additionally depends on the muscle’s diameter. Moreover, the effect of this factor on the tip steering capability of the robot is influenced by the density of the material the robot is fabricated from.

The rest of this paper is structured as follows: in Sec. 2 we describe the soft growing robot prototype; in Sec. 3 we report its characterization procedure; in Sec. 4 we discuss the obtained results; in Sec. 5 we draw conclusions and indicate directions for future research on the topic.

2 Soft Growing Robot Prototype Description

The soft growing robot considered in this work is made up of an everting backbone and two fPAMs glued to diametrically opposite sides. The backbone is inverted such that when pressurized it pulls new material out from its tip causing the robot body to extend by growing (see Fig. 1) [18]. Instead, when pressurized, the laterally attached fPAM contracts and cause a shortening of the backbone side, thus making this to deform and thus steer its tip. Compressed air is typically supplied through a pipe attached to an analog/digital pressure regulator. When in free space, a local constant shortening deformation of the fPAM along the backbone can be observed, thus the whole robot undergoes a constant curvature deformation inducing tip steering (see Fig. 2).

The robot we constructed is made out of a single layer of woven, airtight, silicone coated, rip-stop nylon fabric, commonly used in camping tents and tarps. The rip-stop pattern is simply a plain weave with thicker, reinforcing strands at regular intervals in both the warp and weft direction. The key to the operation of the presented fPAM is fabric bias. The fabric is inextensible along the major thread lines, but is fairly elastic along the fabric bias at a 45° angle to these threads (see Fig. 3). This means that a tube of bias-cut fabric will be elastic, while a tube with a straight or cross grain cut will not. As a result, when the tube is pressurized it expands radially while contracting lengthwise exhibiting a behavior similar to a McKibben muscle [12].

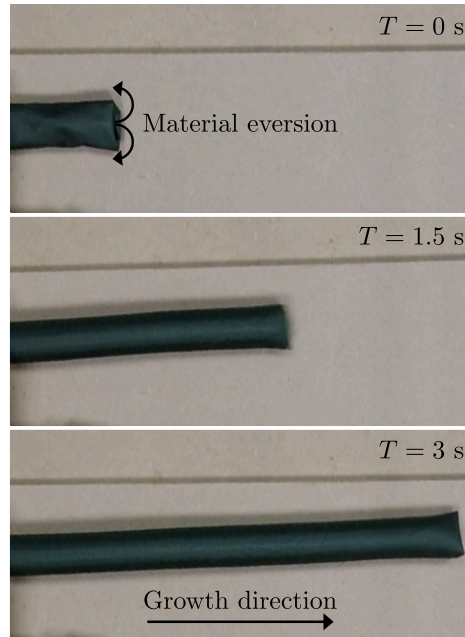


Fig. 1. Timed sequence of pictures showing a soft growing robot extending its body by everting new material from the tip.

However, differently from McKibbens, where the maximum lengthwise contraction depends only upon the angle that the strands of the sheath form with the longitudinal axis, in the considered fabric, where the circumferential expansion is given by the elastic deformation of the material itself, the maximum contraction achievable also depends upon the fPAM cross-section dimensions. Our hypothesis is that a larger circumferential total deformation can be achieved when more material is locally stretched by the internal fluid pressure.

In the next section, we characterize the effects of design parameters on the tip steering capability of the considered soft growing robot prototype.

3 Soft Growing Robot Characterization

The main goal of this work is to characterize the effects of the fPAM and backbone material m , the fPAM diameter d , and the internal backbone pressure p (hereafter denoted to as factors) on the resulting curvature $c = 1/r$ (see Fig. 4) assumed by the robot (hereafter denoted to as metric) given a fixed value of the fPAM internal fluid pressure. To this end, we performed the experiments described in the next section.

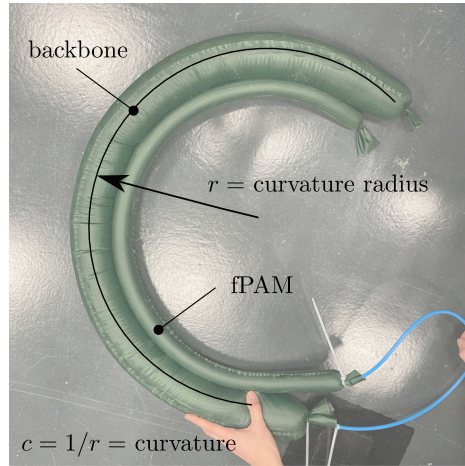


Fig. 2. A fully extended soft growing robot backbone deformed by the contraction of a laterally glued fabric Pneumatic Artificial Muscle (fPAM). Compressed air is supplied through the blue tubing. r = constant curvature steering deformation radius; $c = 1/r$ = constant curvature.

3.1 Experimental Plan

We designed and carried out an experimental campaign considering the variation of the three factors on two pre-defined levels. The numerical values of the two levels of the three factors are given in Table 1 and were opportunely chosen to induce variability in the robot tip steering behavior. A full factorial plan comprising a total of $2^3 = 8$ experiments was defined. Trials were carried out using the experimental setup explained in details in the next section.

For the considered experiments, four soft growing robots (full length = 700 mm) were prototyped to account all the possible combinations of materials with different density (Level 1 = 20 den; Level 2 = 40 den), and fPAM diameter (Level 1 = 25 mm; Level 2 = 45 mm). The two levels of backbone pressure (Level 1 = 0.3 bar; Level 2 = 0.5 bar) did not require the fabrication of additional prototypes.

Table 1. Factors' levels used in the conducted experimental campaign.

| Factor | Symbol | Units | Level 1 | Level 2 |
|-------------------|--------|-------|---------|---------|
| Material | m | den | 20 | 40 |
| fPAM diameter | d | mm | 25 | 45 |
| Backbone pressure | p | bar | 0.3 | 0.5 |

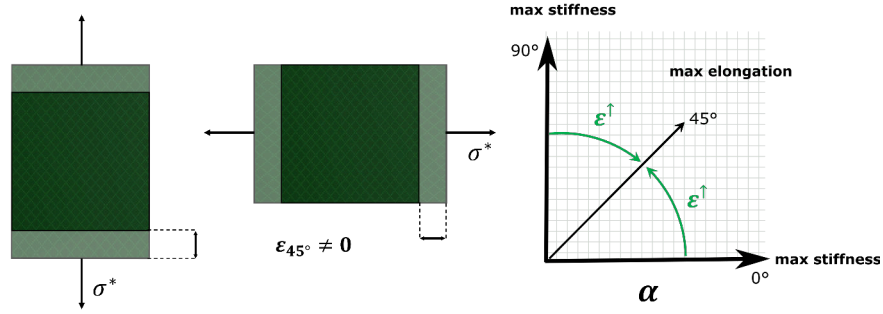


Fig. 3. Drawing of the material elastic deformation as a function of the bias-cut angle α . The maximum elongation ε , for a given internal stress σ^* , is observable when fiber angle $\alpha = 45^\circ$.

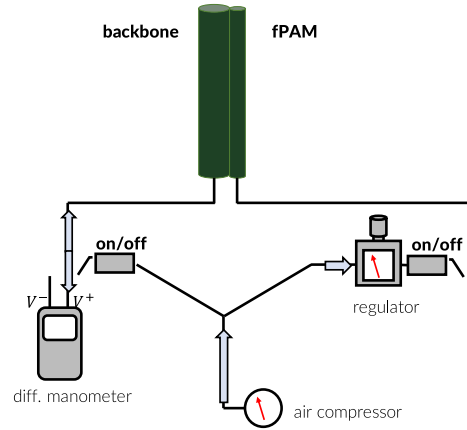


Fig. 4. Schematic of the experimental setup.

3.2 Experimental Setup

The experimental setup implemented for the regulation and the measurement of the fluid pressures in the fPAMs and in the backbone is shown in Fig. 4. The soft growing robot prototypes, built to carry out the experimental campaign, were constituted by one backbone and one fPAM glued to it, exploiting symmetry with respect to the backbone center line. A manometer has been used to measure the air pressure and the air flow in input to the backbone. A pressure regulator, instead, has been used to keep a constant value of pressure of the fluid inside the fPAM (this parameter is, indeed, not varying across the trials). In this way, it is possible to characterize the effect of curvature variation when the pressure inside the backbone varies. In addition, a calibrated camera has been placed in an overhead looking-down configuration to measure the curvature radius of the

robot. This value has been retrieved by manually fitting a circle to the centerline of the robot from the acquired image using the Kinovea software (see Fig. 2).

3.3 Results

The collected data were analyzed with the aim of finding out which combination of design and actuation parameters have statistically significant influence on the performance of the robot (i.e., the tip steering capability, in the considered case).

A three-way ANOVA statistical test was used considering the curvature c of the soft growing robot as dependent parameter, while the backbone's internal pressure p , the fPAM diameter d , and the material m as independent parameters.

Results were obtained by means of the MATLAB Statistics and Machine Learning Toolbox and are reported in Table 2, that shows the three main and the three interaction effects between m , d , and p factors. As it is possible to note, the only factor giving a statistically significant effect ($p < 0.05$) on the chosen curvature metric is the fPAM diameter d . Thus, we can claim that the fPAM diameter is the factor playing the most relevant role among those considered in the design of tip steerable soft-growing robots. Although not statistically significant ($p < 0.05$), the interaction between the material m and the fPAM diameter d shows an interesting effect that will be better discussed in the next section.

4 Discussion

The obtained results are plotted in Fig. 5. In the top graphs, it is possible to see that for a given fPAM diameter d and internal pressure p of the backbone, the less dense material (20 den) achieves greater values of the curvature metric c with respect to the denser material (40 den). This result is expected since the less dense material is in general less stiff to bending deformation. For a given material m and internal pressure of the backbone p , increasing the diameter of the fPAM allows achieving greater values of the curvature deformation c . As explained above, this result is statistically significant and supports our hypothesis. This is given by the fact that larger values of the fPAM cross section determines

Table 2. Analysis of variance results.

| | Df | Sum Sq | Mean Sq | F-Value | p-Value |
|---------|----|-------------|-------------|---------|---------|
| m | 1 | 1.52296e-08 | 1.52296e-08 | 10.54 | 0.1902 |
| d | 1 | 3.41959e-07 | 3.41959e-07 | 236.69 | 0.0413 |
| p | 1 | 1.43625e-07 | 1.43625e-07 | 99.41 | 0.0636 |
| $m * d$ | 1 | 1.62587e-07 | 1.62587e-07 | 112.53 | 0.0598 |
| $m * p$ | 1 | 3.10859e-08 | 3.10859e-08 | 21.52 | 0.1352 |
| $d * p$ | 1 | 4.22775e-09 | 4.22775e-09 | 2.93 | 0.3368 |
| Error | 1 | 1.44477e-09 | 1.44477e-09 | | |
| Total | 7 | 7.00158e-07 | | | |

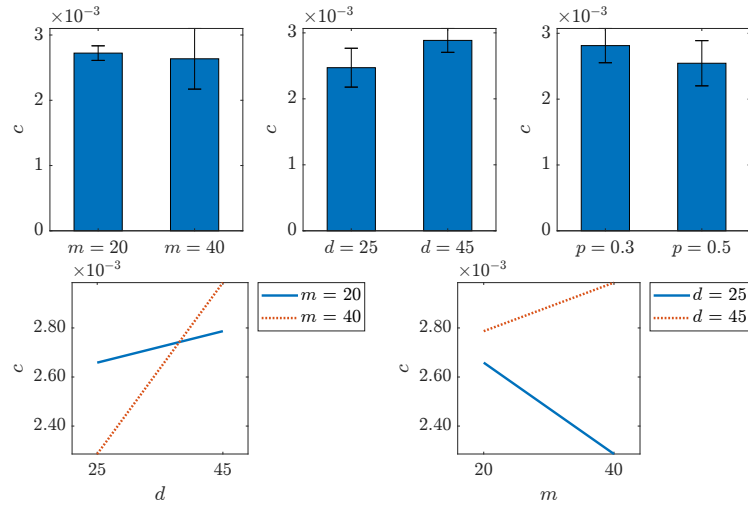


Fig. 5. Top graphs: box plots of the main effects of the material (m), fPAM’s diameter (d), and backbone internal pressure (p). Bottom graphs: plots of the interaction effects between m and d .

greater shortening, and thus allows achieving a higher curvature of the backbone. For a given level of the material m and fPAM diameter d , increasing the internal pressure of the backbone p penalizes the curvature achieved because higher pressures, in general, correspond to higher stiffness of the backbone. In this case, since the fPAM internal pressure is kept constant, the actuator exerts a constant force to deform the backbone, and this results in a lower curvature achieved.

Although not statistically significant ($p = 0.0598$) it is worth to discuss the interaction effect between m and d . This is shown in the bottom graphs of Fig. 5. In the case of $d = 25$ mm better results in terms of achieved curvature can be seen going from the denser to the less dense material. However, this trend is inverted when $d = 45$ mm: the 40 den material exhibits a higher value of the curvature. This effect can also be observed when the material is fixed and the fPAM diameter varies. This can be better appreciated looking at the graphs in Fig. 6, where the inversion of the trend commented above is clearer. Finally, from the same plots it is possible to see that for the denser material the range of curvature values is wider with respect to the less dense material. This explains the less variance observed in the plots of Fig. 5 and is representative of the fact that the less dense material is less dependent on the internal pressure of the backbone.

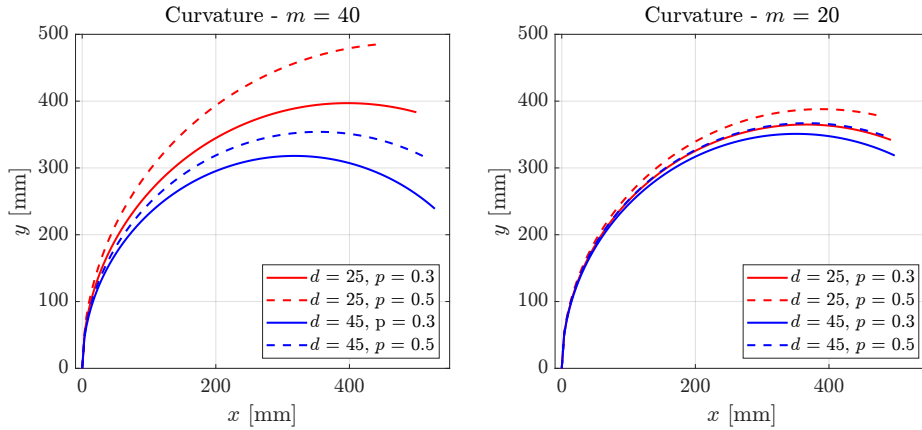


Fig. 6. In the graphs, lines represent the robot curved configurations assumed with the two considered materials when fPAM diameter and backbone internal pressure vary. Left: $m = 40$ den material; Right: $m = 20$ den material.

5 Conclusions

In this paper, we analyzed the effect of design parameters on the tip steering capabilities of fPAM-actuated soft growing robots. More specifically, we considered the variability of material, fPAM diameter, and backbone internal pressure and statistically quantify the effect on the curvature achieved by the robot when a constant fPAM input pressure is supplied. In the considered setting, we found a statistically significant main effect ($p < 0.05$) of the fPAM diameter and a relevant interaction effect between this and the material factor. These findings provide useful guidelines for the design of fabric-based PAM-actuated soft growing robots. Indeed, when the objective is to maximize the curvature of the robot, it is convenient to fabricate fPAMs with larger diameters, while the material and the internal backbone pressure can instead be selected according to other criteria, e.g. cost. However, it is worth to consider that, in view of the discussed interaction effect between the material m and fPAM diameter d , when larger fPAM diameters are selected, the denser material allows achieving higher curvatures.

Although experiments were conducted in a controlled laboratory setup, other external effects not considered here, such as ground friction and manual pre-tension impressed to the fPAMs during fabrication, may have had a non-negligible influence on the presented results. Our aim is to further investigate and reduce these effects in future studies on this topic.

Acknowledgments

This work was supported by the BIOIC project (Bioinspired soft robotic systems for cognitive production). <https://www.bioic.unina.it/>

References

1. Abrar, T., Putzu, F., Ataka, A., Godaba, H., Althoefer, K.: Highly manoeuvrable eversion robot based on fusion of function with structure. In: 2021 IEEE International Conference on Robotics and Automation (ICRA). pp. 12089–12096 (2021). <https://doi.org/10.1109/ICRA48506.2021.9561873>
2. Ataka, A., Abrar, T., Putzu, F., Godaba, H., Althoefer, K.: Model-based pose control of inflatable eversion robot with variable stiffness. *IEEE Robotics and Automation Letters* **5**(2), 3398–3405 (2020). <https://doi.org/10.1109/LRA.2020.2976326>
3. Berthet-Rayne, P., Sadati, S.M.H., Petrou, G., Patel, N., Giannarou, S., Leff, D.R., Bergeles, C.: Mammobot: A miniature steerable soft growing robot for early breast cancer detection. *IEEE Robotics and Automation Letters* **6**(3), 5056–5063 (July 2021). <https://doi.org/10.1109/LRA.2021.3068676>
4. Blumenschein, L.H., Gan, L.T., Fan, J.A., Okamura, A.M., Hawkes, E.W.: A tip-extending soft robot enables reconfigurable and deployable antennas. *IEEE Robotics and Automation Letters* **3**(2), 949–956 (2018)
5. Blumenschein, L.H., Okamura, A.M., Hawkes, E.W.: Modeling of bioinspired apical extension in a soft robot. In: *Biomimetic and Biohybrid Systems*. pp. 522–531. Springer International Publishing, Cham (2017)
6. Blumenschein, L.H., Koehler, M., Usevitch, N.S., Hawkes, E.W., Rucker, D.C., Okamura, A.M.: Geometric solutions for general actuator routing on inflated-beam soft growing robots. *IEEE Transactions on Robotics* pp. 1–21 (2021). <https://doi.org/10.1109/TRO.2021.3115230>
7. Blumenschein, L.H., Usevitch, N.S., Do, B.H., Hawkes, E.W., Okamura, A.M.: Helical actuation on a soft inflated robot body. In: 2018 IEEE International Conference on Soft Robotics (RoboSoft). pp. 245–252 (2018). <https://doi.org/10.1109/ROBOSOFT.2018.8404927>
8. Campbell, S.: The robotics revolution will be soft: Soft robotics proliferate-along with their sources of inspiration. *IEEE Pulse* **9**(3), 19–24 (May 2018). <https://doi.org/10.1109/MPUL.2018.2814240>
9. Coad, M.M., Blumenschein, L.H., Cutler, S., Reyna Zepeda, J.A., Naclerio, N.D., El-Hussieny, H., Mehmood, U., Ryu, J.H., Hawkes, E.W., Okamura, A.M.: Vine robots: Design, teleoperation, and deployment for navigation and exploration. *IEEE Robotics Automation Magazine* **27**(3), 120–132 (Sep 2020). <https://doi.org/10.1109/MRA.2019.2947538>
10. Coad, M.M., Thomasson, R.P., Blumenschein, L.H., Usevitch, N.S., Hawkes, E.W., Okamura, A.M.: Retraction of soft growing robots without buckling. *IEEE Robotics and Automation Letters* **5**(2), 2115–2122 (April 2020). <https://doi.org/10.1109/LRA.2020.2970629>
11. Exarchos, I., Do, B.H., Stroppa, F., Coad, M.M., Okamura, A.M., , Liu, C.K.: Task-specific design optimization and fabrication for inflated-beam soft robots with growable discrete joints. In: *IEEE International Conference on Robotics and Automation* (2022), <http://arxiv.org/abs/2103.04942>
12. Gaylord, R.H.: Fluid actuated motor system and stroking device (US Patent 2, 844, 126, Jul 22, 1958)
13. Greer, J.D., Morimoto, T.K., Okamura, A.M., Hawkes, E.W.: A Soft, Steerable Continuum Robot That Grows via Tip Extension. *Soft Robot* **6**(1), 95–108 (02 2019)
14. Greer, J.D., Blumenschein, L.H., Alterovitz, R., Hawkes, E.W., Okamura, A.M.: Robust navigation of a soft growing robot by exploiting con-

- tact with the environment. *The International Journal of Robotics Research* **39**(14), 1724–1738 (2020). <https://doi.org/10.1177/0278364920903774>, <https://doi.org/10.1177/0278364920903774>
15. Greer, J.D., Blumenschein, L.H., Okamura, A.M., Hawkes, E.W.: Obstacle-aided navigation of a soft growing robot. In: 2018 IEEE International Conference on Robotics and Automation (ICRA). pp. 4165–4172 (May 2018). <https://doi.org/10.1109/ICRA.2018.8460777>
 16. Greer, J.D., Morimoto, T.K., Okamura, A.M., Hawkes, E.W.: Series pneumatic artificial muscles (spams) and application to a soft continuum robot. In: 2017 IEEE International Conference on Robotics and Automation (ICRA). pp. 5503–5510 (May 2017). <https://doi.org/10.1109/ICRA.2017.7989648>
 17. Haggerty, D.A., Banks, M., Curtis, P.C., Mezić, I., Hawkes, E.W.: Modeling, reduction, and control of a helically actuated inertial soft robotic arm via the koopman operator. *ArXiv abs/2011.07939* (2020)
 18. Hawkes, E.W., Blumenschein, L.H., Greer, J.D., Okamura, A.M.: A soft robot that navigates its environment through growth. *Science Robotics* **2**(8), eaan3028 (2017). <https://doi.org/10.1126/scirobotics.aan3028>, <https://www.science.org/doi/abs/10.1126/scirobotics.aan3028>
 19. Jeong, S.G., Coad, M.M., Blumenschein, L.H., Luo, M., Mehmood, U., Kim, J.H., Okamura, A.M., Ryu, J.H.: A tip mount for transporting sensors and tools using soft growing robots. In: 2020 IEEE/RSJ International Conference on Intelligent Robots and Systems (IROS). pp. 8781–8788 (Oct 2020). <https://doi.org/10.1109/IROS45743.2020.9340950>
 20. Li, M., Obregon, R., Heit, J.J., Norbash, A., Hawkes, E.W., Morimoto, T.K.: Vine catheter for endovascular surgery. *IEEE Transactions on Medical Robotics and Bionics* **3**(2), 384–391 (May 2021). <https://doi.org/10.1109/TMRB.2021.3069984>
 21. Liu, Y.P., Wang, C.G., Tan, H.F., Wade, M.K.: The interactive bending wrinkling behaviour of inflated beams. *Proceedings of the Royal Society A: Mathematical, Physical and Engineering Sciences* **472**(2193), 20160504 (2016). <https://doi.org/10.1098/rspa.2016.0504>, <https://royalsocietypublishing.org/doi/abs/10.1098/rspa.2016.0504>
 22. Naclerio, N.D., Hawkes, E.W.: Simple, low-hysteresis, foldable, fabric pneumatic artificial muscle. *IEEE Robotics and Automation Letters* **5**(2), 3406–3413 (April 2020). <https://doi.org/10.1109/LRA.2020.2976309>
 23. Naclerio, N.D., Karsai, A., Murray-Cooper, M., Ozkan-Aydin, Y., Aydin, E., Goldman, D.I., Hawkes, E.W.: Controlling subterranean forces enables a fast, steerable, burrowing soft robot. *Science Robotics* **6**(55), eabe2922 (2021). <https://doi.org/10.1126/scirobotics.abe2922>, <https://www.science.org/doi/abs/10.1126/scirobotics.abe2922>
 24. Rus, D., Tolley, M.T.: Design, fabrication and control of soft robots. *Nature* **521**(7553), 467–475 (May 2015)
 25. Selvaggio, M., Ramirez, L.A., Naclerio, N.D., Siciliano, B., Hawkes, E.W.: An obstacle-interaction planning method for navigation of actuated vine robots. In: 2020 IEEE International Conference on Robotics and Automation (ICRA). pp. 3227–3233 (May 2020). <https://doi.org/10.1109/ICRA40945.2020.9196587>
 26. Slade, P., Gruebele, A., Hammond, Z., Raitor, M., Okamura, A.M., Hawkes, E.W.: Design of a soft catheter for low-force and constrained surgery. In: IEEE/RSJ International Conference on Intelligent Robotic Systems. pp. 174–180 (2017)
 27. Stroppa, F., Luo, M., Yoshida, K., Coad, M.M., Blumenschein, L.H., Okamura, A.M.: Human interface for teleoperated object manipula-

- tion with a soft growing robot. In: 2020 IEEE International Conference on Robotics and Automation (ICRA). pp. 726–732 (May 2020). <https://doi.org/10.1109/ICRA40945.2020.9197094>
28. Wang, S., Zhang, R., Haggerty, D.A., Naclerio, N.D., Hawkes, E.W.: A dexterous tip-extending robot with variable-length shape-locking. In: 2020 IEEE International Conference on Robotics and Automation (ICRA). pp. 9035–9041 (May 2020). <https://doi.org/10.1109/ICRA40945.2020.9197311>
 29. Watson, C., Obregon, R., Morimoto, T.K.: Closed-loop position control for growing robots via online jacobian corrections. *IEEE Robotics and Automation Letters* **6**(4), 6820–6827 (Oct 2021). <https://doi.org/10.1109/LRA.2021.3095625>